Estimation of Fracture Stiffness, In Situ Stresses, and Elastic Parameters of Naturally Fractured Geothermal Reservoirs

Shike Zhang[1]; Shunde Yin, M.ASCE[2]; and Yanguang Yuan[3]

Abstract: Knowledge of fracture stiffness, in situ stresses, and elastic parameters is essential to the development of efficient well patterns and enhanced geothermal systems. In this paper, an artificial neural network (ANN)–genetic algorithm (GA)-based displacement back analysis is presented for estimation of these parameters. Firstly, the ANN model is developed to map the nonlinear relationship between the fracture stiffness, in situ stresses, elastic parameters, and borehole displacements. A two-dimensional discrete element model is used to conduct borehole stability analysis and provide training samples for the ANN model. The GA is used to estimate the fracture stiffness (k_n, K_s), horizontal in situ stresses (σ_H, σ_h), and elastic parameters (E, v) based on the objective function that is established by combining the ANN model with monitoring displacements. Preliminary results of a numerical experiment show that the ANN-GA-based displacement back analysis method can effectively estimate the fracture stiffness, horizontal in situ stresses, and elastic parameters from borehole displacements during drilling in naturally fractured geothermal reservoirs. **DOI:** 10.1061/(ASCE)GM.1943-5622.0000380.

Author keywords: Enhanced geothermal systems; Fracture stiffness; In situ stresses; Elastic parameters; Borehole displacements; Artificial neural network (ANN)–genetic algorithm (GA) model.

Introduction

In the geothermal energy industry, information on fracture stiffness, in situ stresses, and elastic parameters of naturally fractured geothermal reservoirs is vital for safe massive extraction of fluids, wellbore stability analysis, hydraulic fracturing design, and coupled geomechanics-reservoir simulation. Fracture stiffness describes the stress-deformation characteristics of fracture, in situ stresses describe the state that the formation is subject to by initial compressive stresses prior to any artificial activity, and elastic parameters reflect the stress-strain characteristics of rock. Accurate and low-cost information on these parameters is crucial for economic drilling and production of heat from an enhanced geothermal system (EGS) (Rutqvist and Stephansson 2003; Häring et al. 2008).

In naturally fractured geothermal reservoirs, natural fracture characterization is essential for recovery strategy design and borehole-design optimization (Magnusdottir and Horne 2011). The natural fracture pattern and its initial aperture are relatively straightforward to be obtained by using direct methods (e.g., cores and cuttings) and/or indirect methods (e.g., borehole images, geophysical logs, flow logs, and temperature logs) (Kubik and Lowry 1993; Dezayes et al. 2010). Recently, Magnusdottir and Horne (2011) investigated subsurface electrical resistivity to infer the dimensions and topology of a fracture network in geothermal fields. Juliusson (2012) studied heat production data to characterize the fracture network layout of geothermal reservoirs. The works of Main et al. (1990) and Watanabe and Takahashi (1995) have shown that fracture patterns of naturally fractured geothermal reservoirs are commonly fractal.

However, estimation of normal and shear stiffness of a natural fracture is difficult or even impossible, especially for normal stiffness of a fracture (Hesler et al. 1990; Alber and Hauptfleisch 1999; Gokceoglu et al. 2004). The two parameters are indispensable in designing a borehole recovery strategy and modeling fractured geothermal reservoirs (McDermott and Kolditz 2006; Sharifzadeh and Karegar 2007; Koh et al. 2011). Some researchers used laboratory methods to estimate these parameters. Huang et al. (1993) investigated fracture shear stiffness using a direct shear apparatus under a boundary condition of constant normal load. This method, however, is not suitable for deep underground rock formations. To overcome this limitation, Jiang et al. (2004) developed an automated servocontrolled direct shear apparatus to determine fracture shear stiffness by assuming a constant normal stiffness condition. In practice, it is more difficult to obtain information on normal stiffness than shear stiffness of a fracture. Because of various limitations of laboratory methods, some researchers choose to perform a back analysis to estimate these parameters by using different numerical models (Alber and Hauptfleisch 1999; Nassir et al. 2010; Morris 2012; Jing and Stephansson 2007; Noorzad and Aminpoor 2008). Jiang et al. (2009) investigated the relationship between fracture transmissivity and depth, and used information of depth-dependent transmissivity to estimate fracture normal stiffness. A limitation of these approaches is that they require precise knowledge of in situ stresses and rock elastic parameters.

In general, the orientations of the in situ stresses are assumed to coincide with the vertical and horizontal directions. Bell and Gough (1979) reduced the stress tensor to three components: (1) the vertical stress magnitude, σ_v; (2) the maximum horizontal stress, σ_H; and (3) the minimum horizontal stress, σ_h. By integration of rock densities from the surface to the depth of interest, the vertical stress magnitude can be easily calculated (Haftani et al. 2008). For the two horizontal in situ stresses, however, it is generally difficult to determine

[1]Assistant Professor, School of Civil Engineering and Architecture, Anyang Normal Univ., Anyang, Henan 455000, China. E-mail: shikezhang128@gmail.com

[2]Assistant Professor, Dept. of Chemical and Petroleum Engineering, Univ. of Wyoming, Laramie, WY 82071 (corresponding author). E-mail: syin@uwyo.edu

[3]Professor, BitCan Geosciences and Engineering Inc., Suite 217-2770, 3 Ave. NE, Calgary, AB, Canada T2A 2L5. E-mail: yuany@bitcange.com

Note. This manuscript was submitted on August 15, 2013; approved on December 11, 2013; published online on December 13, 2013. Discussion period open until September 3, 2014; separate discussions must be submitted for individual papers. This paper is part of the ***International Journal of Geomechanics***, © ASCE, ISSN 1532-3641/04014033(9)/$25.00.

by simple calculation. Hydraulic fracturing methods (Haimson and Fairhurst 1969; White et al. 2002; Sheridan and Hickman 2004; Haftani et al. 2008) and an inversion method based on wellbore deformation (Moos and Zoback 1990; Valley and Evans 2007; Zoback 2007) are popular methods for the determination of maximum and minimum horizontal in situ stresses (Sheridan and Hickman 2004).

However, investigations (Rutqvist and Stephansson 1996; Yang et al. 1997; Hossain et al. 2002) have shown that hydraulic fracturing methods are difficult to conduct or are ineffective for the estimation of horizontal in situ stresses of naturally fractured geothermal reservoirs at a great depth because of the higher horizontal in situ stresses and preexisting natural fractures. Other methods, such as laboratory rock strength tests, in situ pore pressure measurements, wireline logging data, and the acoustic emission method (Amadei and Stephansson 1997), can also be used to obtain the horizontal in situ stresses under the assumption that rock elastic parameters are known constants. However, these may only serve as a complement to hydraulic fracturing or borehole deformation methods and are less accurate (Ljunggren et al. 2003; Sheridan and Hickman 2004). Estimating natural fracture stiffness, in situ stresses, and elastic parameters of naturally fractured geothermal reservoirs simultaneously, therefore, still remains challenging as a geomechanics problem (Gokceoglu et al. 2004; Jiang et al. 2009).

In this paper, a novel method that can simultaneously identify the fracture stiffness, horizontal in situ stresses, and elastic parameters using field monitoring data is presented. This proposed method is the artificial neural network (ANN)–genetic algorithm (GA)-based displacement back analysis method, which has been successfully used in rock mechanics and engineering for parameter identification and optimum design (Feng et al. 2000, 2004; Pichler et al. 2003; Zhang and Yin 2013). This paper takes advantage of monitoring borehole displacements at multiple points of location during drilling to identify the previously mentioned parameters because the wellbore displacements are easily measured by International Society for Rock Mechanics–suggested methods (Li et al. 2013a, b). The remainder of the paper is structured as follows. First, the two-dimensional numerical model for sample generation and validation of identified parameters is described. Then, the hybrid ANN-GA model for back analysis is presented. Finally, the results of a numerical experiment study are presented and discussed.

Forward Model

Discrete Element Method Model Based on a Thermoporoelastoplasticity Framework

Subsurface drilling in oil and gas development involves a strong coupling among fluid flow, heat transfer, and rock deformation (Yuan et al. 1995; Yin et al. 2010). The coupling effect is also significant in drilling through fractured geothermal reservoirs (Koh et al. 2011). The deformation of a fractured rock formation is composed of both the elastic and plastic deformation of intact rock and displacements along and across fracture (Barton et al. 1985). *Universal Distinct Element Code (UDEC) 5.0* has been successfully used in the numerical modeling of borehole behavior in fractured rock masses (Chen et al. 2003; Nicolson and Hunt 2004), and therefore is used in this paper to conduct the coupled thermal-hydraulic-mechanical (THM) analysis in which fracture conductivity is dependent on the fracture properties. Elastoplastic deformation of intact rock is represented by the Mohr-Coulomb criterion and nonassociated flow rule in a thermoporoelastoplasticity framework. The deformation of the fractures follows the Coulomb slip model.

Stress and Strain of Intact Rock

The constitutive relation for the nonisothermal single phase fluid flow through deformable fractured media incorporating the concept of effective stress can be expressed as (Lewis and Schrefler 1998)

$$d\boldsymbol{\sigma}' = D^{ep}(d\boldsymbol{\varepsilon} - d\boldsymbol{\varepsilon}^p) - \mathbf{m}\delta_{ij}\frac{18KG}{3K+4G}\beta dT + \mathbf{m}\,\alpha dp \quad (1)$$

where $d\boldsymbol{\sigma}'$ = effective stress increment; $d\boldsymbol{\varepsilon}$ = total strain increment; $d\boldsymbol{\varepsilon}^p$ = plastic strain increment; $\mathbf{m} = [1, 1, 0]^T$; K = bulk modulus; G = shear modulus; β = thermal expansion coefficient; dT = temperature increment; α = Biot's coefficient; and dp = pore pressure increment. The elastoplastic stress-strain matrix, $\mathbf{D}^{ep}$ is given by

$$\mathbf{D}^{ep} = \mathbf{D}^e - \frac{\mathbf{D}^e \dfrac{\partial Q}{\partial \boldsymbol{\sigma}'}\left(\dfrac{\partial F}{\partial \boldsymbol{\sigma}'}\right)^T \mathbf{D}^e}{-\dfrac{\partial F}{\partial \kappa}\left(\dfrac{\partial F}{\partial \boldsymbol{\varepsilon}^p}\right)^T \dfrac{\partial Q}{\partial \boldsymbol{\sigma}'} + \left(\dfrac{\partial F}{\partial \boldsymbol{\sigma}'}\right)^T \mathbf{D}^e \dfrac{\partial Q}{\partial \boldsymbol{\sigma}'}} \quad (2)$$

$$\mathbf{D}^e = \frac{E}{(1+\nu)(1-2\nu)}\begin{bmatrix} 1-\nu & \nu & 0 \\ \nu & 1-\nu & 0 \\ 0 & 0 & \dfrac{1-2\nu}{2} \end{bmatrix} \quad (3)$$

where E = Young's modulus; ν = Poisson's ratio; κ = hardening parameter; F = yield function; and Q = plastic potential function.

The yield function F for the linear Mohr-Coulomb yield criterion can be expressed as

$$F = \sigma_1' - \sigma_3' \frac{1+\sin\varphi}{1-\sin\varphi} + 2c\sqrt{\frac{1+\sin\varphi}{1-\sin\varphi}} \quad (4)$$

where σ_1', σ_3' = maximum effective principal stress and minimum effective principal stress, respectively; φ = friction angle; and c = cohesion.

A nonassociated flow rule is adopted to simulate the dilatant behavior of rock, and the plastic potential function Q can be expressed as

$$Q = \sigma_1' - \sigma_3' \frac{1+\sin\psi}{1-\sin\psi} \quad (5)$$

where ψ = dilation angle.

Facture Stiffness and Fluid Flow in Fracture

According to Goodman (1970), the normal stiffness k_n and shear stiffness k_s are formulated as follows:

$$k_n = \frac{d\sigma_n'}{du_n} \quad (6)$$

$$k_s = \frac{d\sigma_s'}{du_s} \quad (7)$$

where $d\sigma_n'$ and $d\sigma_s'$ = effective normal and shear stress increments, respectively; and du_n and du_s = increments in normal and shear displacement, respectively.

At edge-to-edge contact, according to the cubic law of flow in fractures (Witherspoon et al. 1980), the flow rate in a single fracture of length l subject to a pressure difference of dp is calculated by

$$q = -\frac{a^3}{12\mu}\frac{dp}{l} \tag{8}$$

where μ = dynamic viscosity. The contact hydraulic aperture, a, is given by the following relationship:

$$a = a_o + u_n \tag{9}$$

where a_o = initial fracture aperture; and u_n = fracture normal displacement.

In the case of a corner-to-corner or corner-to-edge contact, the flow rate is given by

$$q = -k_c dp \tag{10}$$

where k_c = contact permeability factor related to the geometry of a domain.

Heat Transfer in Rock Mass

Based on Fourier's law (Abdallah et al. 1995), the basic equation of conductive heat transfer can be written as

$$Q_i = -k_{ij}\frac{\partial T}{\partial x_j} \tag{11}$$

where Q_i = flux in the i-direction; k_{ij} = thermal conductivity tensor; and T = temperature.

Also, for any mass, the change in temperature can be expressed as

$$\frac{\partial T}{\partial t} = \frac{Q_{\text{net}}}{C_p M} \tag{12}$$

where Q_{net} = net heat flow into mass; C_p = specific heat; and M = mass.

Samples Generation for ANN

As shown in Fig. 1, a vertical borehole drilled through a geothermal reservoir at a depth of 2,000 m is considered a two-dimensional plane strain problem. The initial pore pressure of the formation is $P_o = 20$ MPa. The initial temperature of the formation is $T_o = 100°\text{C}$. The problem domain is subjected to an in situ vertical stress of $\sigma_v = 40.0$ MPa (out of plane). The maximum horizontal in situ stress, σ_H, is aligned with the x-direction, and the minimum horizontal in situ stress, σ_h, is aligned with the y-direction. A fluid pressure of $P_w = 28$ MPa and a temperature of $T_w = 80°\text{C}$ are applied to the borehole wall when the borehole is drilled. A vertical borehole through a geothermal reservoir can be drilled by using commercially available positive displacement motors (PDMs). Many conventional drillstring components, such as drillpipe floats and mechanical drilling jars, can be used to drill a well at a depth of 2,000 m (Brittenham et al. 1982).

As shown in Fig. 2, the domain of the problem studied is based on a pattern of random polygonal fractures, where k_n and k_s are the normal and shear stiffness of a fracture, respectively, and E and v are Young's modulus and Poisson's ratio, respectively. Table 1 gives the input data used in the numerical model. These properties are mainly obtained from Chen et al. (2003) and *UDEC*.

Based on the forward model described in the previous sections, the training and testing samples for the ANN model will be created. The samples are composed of input and output parameters. There are six input parameters for the ANN model: the fracture stiffness (k_n, k_s), horizontal in situ stresses (σ_H, σ_h), and elastic parameters

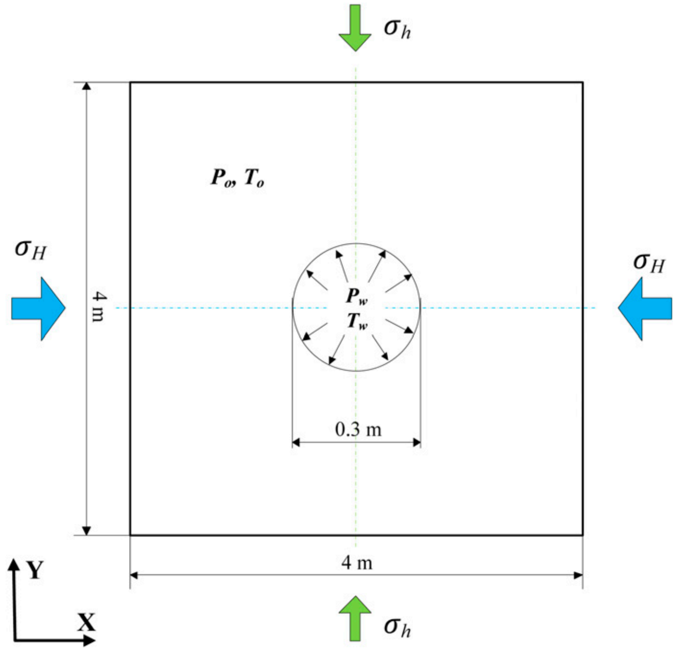

Fig. 1. Borehole geometry and problem domain

(E, v). There are 14 dependent variables considered as ANN outputs: x-direction displacements and y-direction displacements at multiple locations on the wellbore wall, as shown in Figs. 3(a and b).

To generate these samples, the forward model applied at $t = 3$ h with a different fracture stiffness, horizontal in situ stresses, and elastic parameters (i.e., input parameters) is used to obtain borehole displacements at monitoring points (i.e., output parameters) (see Supplemental Data).

Back Analysis Methodology

Artificial Neural Network

McCulloch and Pitts (1943) originally developed the ANN in the 1940s. A fully connected ANN consists of a large number of nodes and weights between the nodes. Each node besides the input nodes is a processing element (or neuron) by using an activation function. The network itself is a type of natural algorithm or logical expression and allows for self-learning, self-organization, and parallel processing. The ANN can be used to analyze large numbers of data and find patterns and relationships from these data so that it is often considered the modeling tools of linear and/or nonlinear statistical data for solving a practical engineering problem. Fig. 4 illustrates a single artificial neuron with a node threshold, b, connection weights, w_i ($i = 1, 2, \ldots, n$), and a transfer function $y^{(j)} = f[x^{(j)}]$. For each pattern j ($j = 1, 2, \ldots, m$), all patterns can be expressed in matrix notation as (Nikravesh et al. 2003)

$$x^{(j)} = x_1^{(j)}w_1 + x_2^{(j)}w_2 + \cdots + x_n^{(j)}w_n + b_j \tag{13}$$

Next, ANN-predicted displacements can be given by a transfer function

$$Y = f(X)w + b \tag{14}$$

In this mathematical model, X represents inputs with weights and thresholds and Y represents predicted outputs. Both the mean square

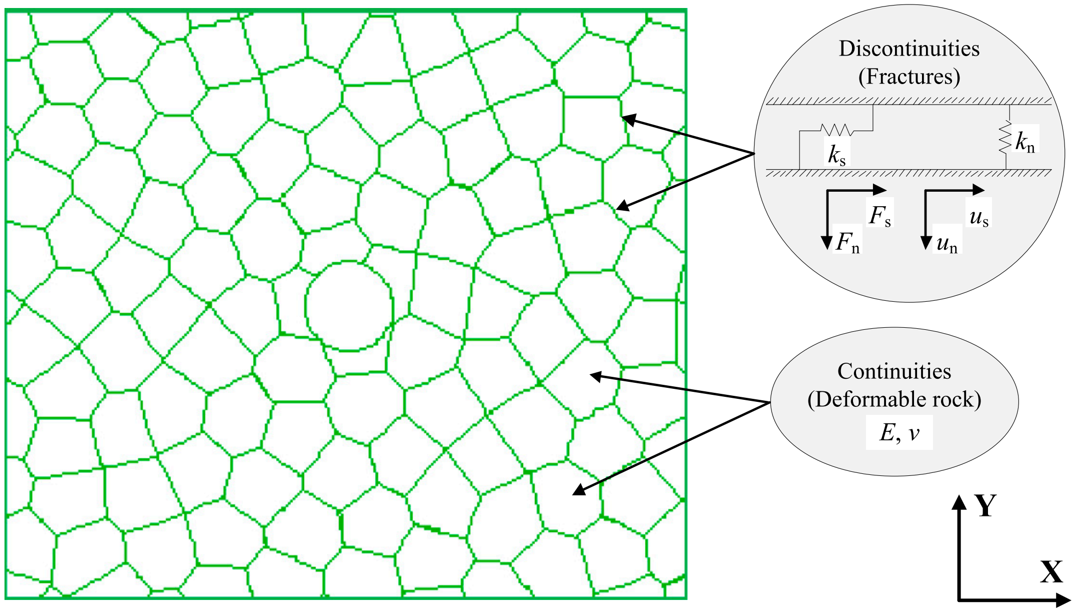

Fig. 2. Pattern and properties of fracture and intact rock in numerical model

Table 1. Input Data for Numerical Modeling

Variable	Value
Intact rock	
Density	2,500 kg/m^3
Cohesion	6.3 MPa
Friction angle	32 degrees
Dilation angle	10 degrees
Tensile strength	2.07 MPa
Fracture	
Permeability factor	83.3 $Pa^{-1}\,s^{-1}$
Friction angle	32 degrees
Residual aperture	0.25 mm
Zero normal stress aperture	0.5 mm
Cohesion	0 MPa
Tensile strength	0 MPa
Fluid and thermal	
Density	1,030 kg/m^3
Bulk modulus	2.0 GPa
Cohesion	0.1 Pa
Specific heat	775 J/kg degrees Celsius
Expansion coefficient	5.0×10^{-6} 1/degrees Celsius
Conductivity	0.25 W/m degrees Celsius

error (MSE) and correlation coefficient (R-value) are applied in this study to the performance evaluation of such an ANN model (Sahoo and Ray 2006).

The MSE is defined as the average sum of squares of the difference between targets and ANN-predicted values

$$\mathrm{MSE} = \frac{1}{n}\sum_{i=1}^{n}(Y_i - T_i)^2 \tag{15}$$

where n = number of samples; and Y_i and T_i = predicted values and targets, respectively.

The R-value is obtained by performing a linear regression between the targets and the ANN-predicted values and can be expressed as

$$R = \frac{\sum_{i=1}^{n} t_i y_i}{\sqrt{\sum_{i=1}^{n} t_i^2}\sqrt{\sum_{i=1}^{n} y_i^2}} \tag{16}$$

where n = number of samples; $t_i = T_i - \overline{T}$; and $y_i = Y_i - \overline{Y}$. Once the performance of the ANN model is satisfactory, it will be used to map the linear and/or nonlinear relationship between the inputs and outputs.

Genetic Algorithm

Goldberg (1989) originally introduced the generic form of GA. The GA is a global search and optimization technique based on some principles from the evolution theory (e.g., natural selection and genetics). The technique starts with a set of solutions to the problem. This set of solutions is called the population, and each individual in the population is called a chromosome. These chromosomes are generated by successive iterations and are evaluated based on the objective function. A roulette wheel selection is adopted to implement the selection operator of GA to determine which chromosomes are selected as parents. Parents create the next generations, new chromosomes, which are also called offspring, through crossover and mutation operations. Now $S_i = [s_{i1}, s_{i2}, \ldots, s_{iN}]$ is used to represent chromosome i in a population $i = 1, 2, \ldots, N_{\text{pop\_size}}$. The fitness is $eval(S_i) = f(S_i)$ for each chromosome S_i. Then, total fitness can be calculated for the population by (Gen and Cheng 1997)

$$S = \sum_{i=1}^{N_{\text{pop\_size}}} eval(S_i) \tag{17}$$

The selection probability for each chromosome S_i can be expressed as (Gen and Cheng 1997)

$$P_i = \frac{eval(S_i)}{S} \tag{18}$$

As in any traditional approach for the displacement back analysis, an objective function is needed to be defined when GA is used to search

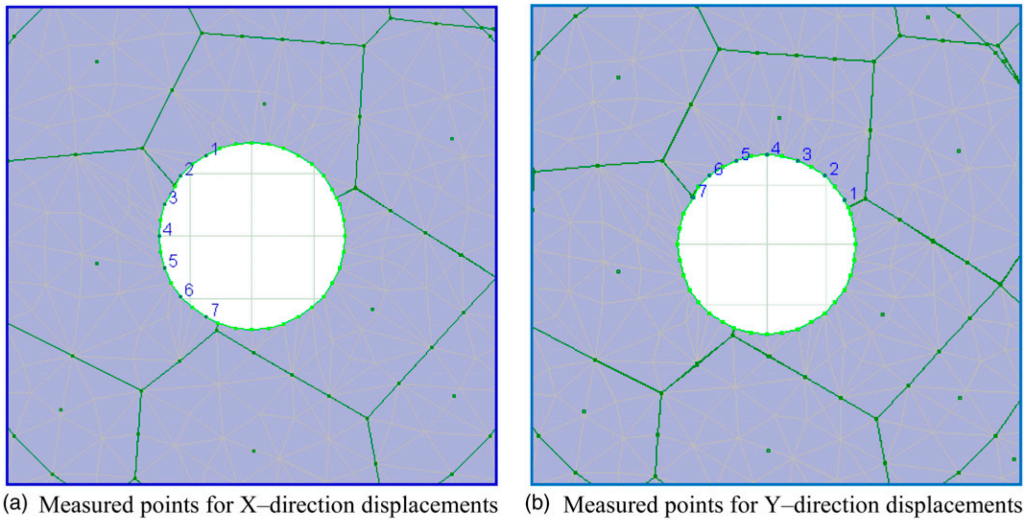

Fig. 3. Locations of monitoring points on borehole wall: (a) measured points for x-direction displacements; (b) measured points for y-direction displacements

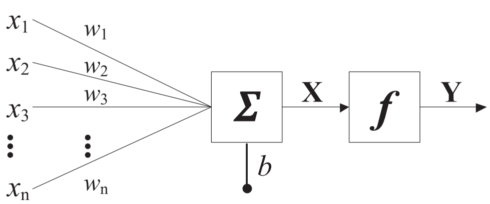

Fig. 4. Schematic of single artificial neuron

the optimal fracture stiffness, horizontal in situ stresses, and elastic parameters in a large search space. The objective function can be defined as

$$\text{fitness} = \min\left[\frac{1}{k}\sum_{j=1}^{k}\left(|Y_j - U_j|\right)\right] \tag{19}$$

where k = number of monitoring points on borehole wall; and Y_j and U_j = predicted displacement and monitoring displacement of the jth monitoring point, respectively.

Hybrid ANN-GA Model

The hybrid ANN-GA model has been successfully used in multiple parameters identification in petroleum engineering (Zhang and Yin 2013). To assess the identified results of the ANN-GA model, the analysis of the objective function value and the comparison of the predicted and calculated displacements with the monitoring displacements are needed, which will be described in the procedure of estimation methodology as follows (see Supplemental Data):

- Step 1: Build a proper ANN by initially determining the network type and its algorithm and the number of hidden layers, number of hidden nodes, and transfer function.
- Step 2: Initialize the weights and biases of the network.
- Step 3: Train the initial network. The training process requires a set of examples of proper network behavior network inputs and target outputs. The weights and biases of the network are iteratively adjusted during training.
- Step 4: If the MSE between the network outputs and targets is satisfied or the epoch is reached, the training process will be stopped. Otherwise, repeat Step 3.
- Step 5: Check the trained ANN model in terms of MSE performance and data regression results.
- Step 6: If both the MSE performance and data regression results are satisfied, the training will end. Then, the best network model topology is saved for GA. Otherwise, go to Step 1.
- Step 7: The initializations of the GA parameter set include population size, $N_{\text{pop\_size}}$, maximum generation, $N_{\text{max\_gen}}$, crossover probability, P_c, mutation probability, P_m, and the range of search space for parameters. In this study, to have an effective implementation of GA, the real number encoding method is employed.
- Step 8: Generate candidate individuals within the given range of parameters. Then, the initial population is generated based on these candidate individuals. Here, each chromosome (individual) represents an initial solution.
- Step 9: Input the generated candidate solutions into the trained and tested ANN model from Step 6. Predicted displacements at the monitoring points are obtained.
- Step 10: Use Eq. (19) to evaluate the fitness of current individuals.
- Step 11: If all individuals have been evaluated, this model will automatically trace the average fitness and the best individual fitness and go to Step 12. Otherwise, go to Step 9.
- Step 12: If the given evolutionary generation is reached or the best individual is obtained, the algorithm terminates and outputs the fracture stiffness, horizontal in situ stresses, elastic parameters, as well as the corresponding displacements. Otherwise, go to Step 13.
- Step 13: Execute genetic operations, including selection, crossover, and mutation. The next generations of selected individuals are obtained based on these genetic operations.
- Step 14: Repeat Step 13 until all $N_{\text{pop\_size}}$ new individuals are generated, which are applied as new individuals (offspring).
- Step 15: Use the generation of the best parent's individual to randomly replace an individual in the offspring.
- Step 16: Take the offspring as the parent and go to Step 9.

Verification of Hybrid ANN-GA Model

To conduct multiple parameters identification, the suitable ANN prediction model mapping the nonlinear relationship among fracture stiffness, horizontal in situ stresses, elastic parameters, and borehole deformation based on the description of inputs and outputs is first obtained. Fig. 5 shows the ANN model applied in this work. Also, 60 samples are applied to train and test the ANN model. By combining the ANN-predicted displacements and monitoring displacements, a suitable objective function is established. Finally, GA is used to search the optimal geomechanical parameters in a large search space based on the objective function. In this work, MSE, R-value, and cross plot on targets versus predicted displacements were used to verify if the ANN model can effectively map the nonlinear relationship among fracture stiffness, horizontal in situ stresses, elastic parameters, and borehole displacements.

Fig. 6 shows the variations of MSE for training, validation, and testing data with iterations. As can be seen, the training stops through 27 training epochs because the validation error starts increasing from 1.728×10^{-8} to 2.087×10^{-8}. For training data, MSE shows a reduction trend with an increase of the training epoch, and the final error value is approximately 0.295×10^{-8}. The results for the test data are also reasonable because the testing set error has similar properties to the validation set error and does not show the significant overfitting in the ANN model.

Fig. 7 shows the linear regression between the network outputs and corresponding targets and R-values for training, validation, testing, and all data. Scatter plots for all the four phases show good correlation and regression values. Correlation coefficients for training, validation, testing, and all data are greater than 0.93, which demonstrates that the ANN model is performing well (Yilmaz and Yuksek 2008).

Fig. 8 shows the cross plot on ANN-predicted displacements versus actual target displacements for the sample sets. This figure is mainly used to illustrate that the degree of accuracy can also be achieved when a complex problem is modeled by ANN. According to assessment results shown previously, it can be seen that the ANN model can accurately map the nonlinear relationship among fracture stiffness, horizontal in situ stresses, elastic parameters, and borehole displacements.

In the displacement back analysis, the parameters of GA are set as follows: maximum generation, $N_{\max\_gen}$, is 400; population size, $N_{\text{pop\_size}}$, is 80; crossover probability, P_c, is 0.5; and mutation probability, P_m, is 0.1. The ranges of parameters identified by a hybrid ANN-GA model are set as follows: fracture normal stiffness, k_n, is 5.0–50.0 GPa/m ; fracture shear stiffness, k_s, is 5.0–50.0 GPa/m; the maximum horizontal in situ stress, σ_H, is 30.0–50.0 MPa; the minimum horizontal in situ stress, σ_h, is 25.0 – 45.0 MPa; Young's modulus, E, is 10.0–50.0 GPa; and Poisson's ratio, v, is 0.15–0.35.

Suppose the x- and y-direction displacements of the monitoring points [see Figs. 3(a and b)] have been obtained, which are listed in Table 2. Then, the hybrid ANN-GA model can be used to estimate the

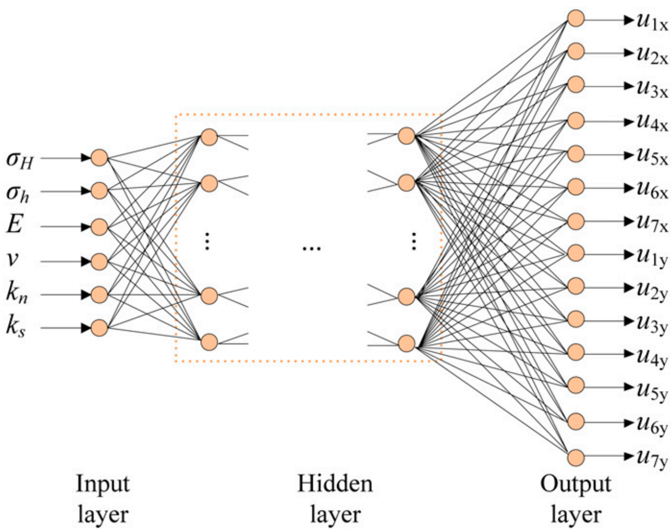

Fig. 5. Neural network model

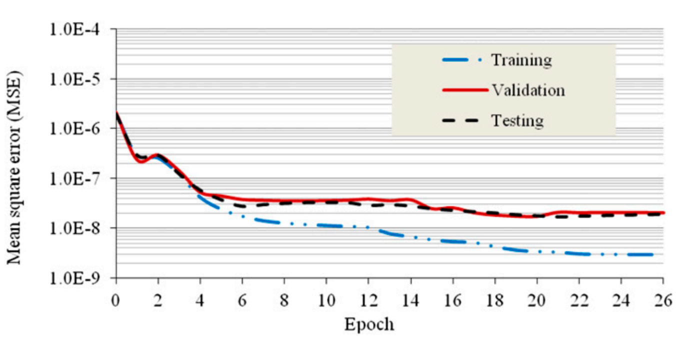

Fig. 6. Variation curves of mean square error with epoch

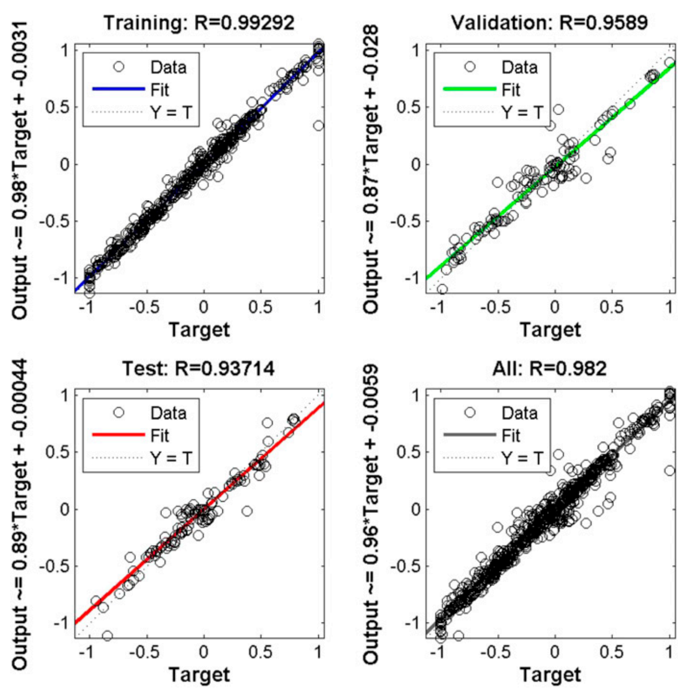

Fig. 7. Linear regressions between network outputs and corresponding targets

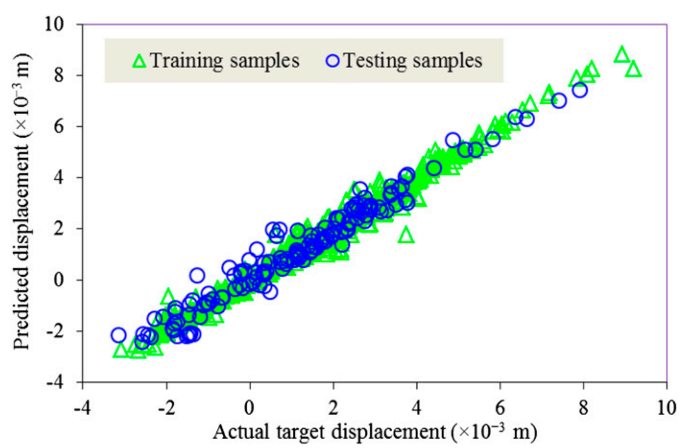

Fig. 8. Cross plot of predicted and actual target displacements

Table 2. Monitoring, Predicted, and Calculated Displacements and Comparison among Them

Number	Displacement at monitoring point ($\times 10^{-3}$ m) Monitoring	ANN predicted	*UDEC* calculated	Absolute error ($\times 10^{-3}$ m) Monitoring and ANN	Monitoring and *UDEC*	Relative error (%) Monitoring and ANN	Monitoring and *UDEC*
u_{x1}	1.606	1.5949	1.512	0.0111	0.094	0.6912	5.8531
u_{x2}	2.361	2.4657	2.184	0.1047	0.177	4.4346	7.4968
u_{x3}	2.317	2.1892	2.147	0.1278	0.17	5.5158	7.3371
u_{x4}	2.05	2.0611	1.887	0.0111	0.163	0.5415	7.9512
u_{x5}	1.549	1.553	1.482	0.004	0.067	0.2582	4.3254
u_{x6}	0.6487	0.5634	0.5931	0.0853	0.0556	13.1494	8.571
u_{x7}	2.431	2.4452	2.254	0.0142	0.177	0.5841	7.281
u_{y1}	3.502	3.4997	3.617	0.0023	0.115	0.0657	3.2838
u_{y2}	4.284	4.2006	4.433	0.0834	0.149	1.94678	3.4781
u_{y3}	5.582	5.5837	5.762	0.0017	0.18	0.0305	3.2247
u_{y4}	5.701	5.7994	5.848	0.0984	0.147	1.726	2.5785
u_{y5}	5.153	5.1142	5.282	0.0388	0.129	0.753	2.5034
u_{y6}	4.283	4.1903	4.422	0.0927	0.139	2.164371	3.2454
u_{y7}	−1.738	−1.7499	−1.686	0.0119	0.052	0.6847	2.9919

geomechanical parameters based on these displacements. To this end, an objective function needs to be established by Eq. (19). Finally, GA can search the optimal solutions within the aforementioned ranges of the parameters to be recognized based on the objective function. After genetic operation of 400 generations of evolution, the ANN-GA model identifies the geomechanical parameters as follows: $k_n = 10.152$ GPa/m, $k_s = 19.2367$ GPa/m, $\sigma_H = 44.5316$ MPa, $\sigma_h = 28.3526$ MPa, $E = 20.7985$ GPa, and $v = 0.2095$.

Correspondingly, the hybrid ANN-GA model based on the displacement back analysis also outputs the x- and y-direction displacements at the monitoring points on the borehole wall. In addition, a comparison numerical experiment in which identified parameters are inputted into the forward *UDEC* model, keeping other parameters at the same values (see Table 1), is conducted to explore the effectiveness of the ANN-GA model. Table 2 also gives the predicted and calculated results as well as their errors. All relative errors are less than 15%, as expected.

Fig. 9 compares the displacement magnitude on monitoring, ANN-predicted, and *UDEC*-calculated displacements at the 14 monitoring points on the borehole wall. Comparison shows that there is a relatively small absolute error in between these displacements. Fig. 10 shows variation curves of objective function values for both the average individual fitness and best individual fitness with generations. The average fitness shows that it has maintained the diversity of individuals when GA was used to search the optimal solutions in a large search space. The final average fitness and final best fitness are very close to the real value of zero. They are approximately 4.89×10^{-5} and 4.83×10^{-5} after genetic operation of 400 generations of evolution, respectively.

From the preceding, it is found that two important evaluation criteria relating to GA optimization are performing excellently, as expected. Results show that the proposed estimation methodology can effectively estimate the fracture stiffness, horizontal in situ stresses, and elastic parameters based on borehole displacements during drilling in naturally fractured geothermal reservoirs.

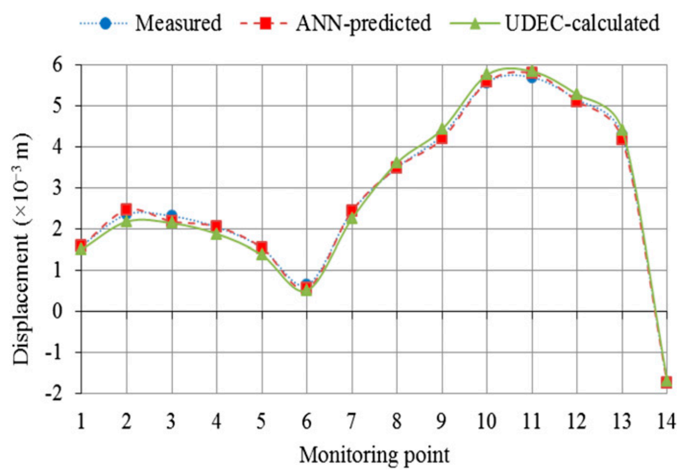

Fig. 9. Comparison of prediction and calculation with measurements

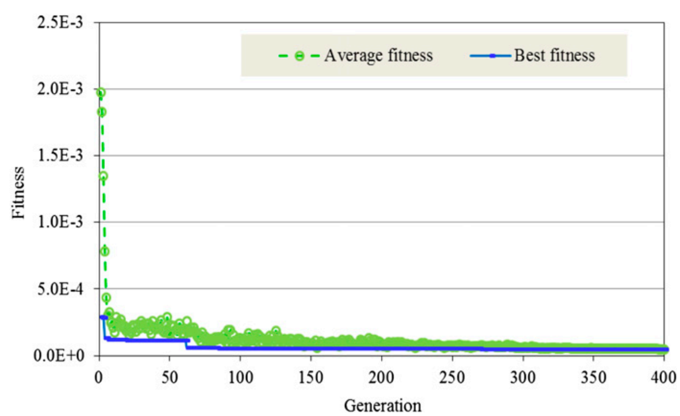

Fig. 10. Variations of value of objective function with generations

Discussions and Conclusions

Discussions

In this paper, an ANN-GA-based displacement back analysis method is employed for the identification of multiple parameters on fracture stiffness, horizontal in situ stresses, and elastic parameters, and *UDEC* is employed to conduct a series of numerical analyses about borehole stability in a thermoporoelastoplasticity framework in naturally fractured geothermal reservoirs. When utilizing the proposed method, it should be noted that the estimation of these parameters cannot be conducted (1) prior to drilling or (2) without wellbore deformation measurement during drilling.

Conclusions

With the ANN-GA model, a hypothetical numerical experiment on borehole deformation when a borehole is drilled in a naturally fractured geothermal reservoir is conducted. Evaluation of the ANN model performance demonstrates that the ANN model can effectively represent the nonlinear relation among fracture stiffness, horizontal in situ stresses, elastic parameters, and borehole displacements. Evaluation of GA performance shows that the GA can rapidly and accurately find the optimal solutions (i.e., k_n, k_s, σ_H, σ_h, E, and v) in a large search space based on the objective function established by combining the ANN model and monitoring displacements. Thus, the proposed method provides an effective tool for multiple geomechanics parameters identification from monitoring data in enhanced geothermal systems.

Acknowledgments

The first and second authors acknowledge the support of the University of Wyoming and BitCan Geosciences and Engineering Inc.

Supplemental Data

Table S1 and Fig. S1 are available online in the ASCE library (www.ascelibrary.org).

References

Abdallah, G., Thoraval, A., Steir, A., and Piguet, J. P. (1995). "Thermal convection of fluid in fractured media." *Int. J. Rock Mech. Min. Sci. Geomech. Abstr.*, 32(5), 481–490.

Alber, M., and Hauptfleisch, U. (1999). "Generation and visualization of microfractures in Carrara marble for estimating fracture toughness, fracture shear and fracture normal stiffness." *Int. J. Rock Mech. Min. Sci.*, 36(8), 1065–1071.

Amadei, B., and Stephansson, O. (1997). *Rock stress and its measurement*, Chapman & Hall, London.

Barton, N., Bandis, S., and Bakhtar, K. (1985). "Strength, deformation and conductivity coupling of rock joints." *Int. J. Rock Mech. Min. Sci. Geomech. Abstr.*, 22(3), 121–140.

Bell, J. S., and Gough, D. I. (1979). "Northeast-southwest compressive stress in Alberta evidence from oil wells." *Earth Planet. Sci. Lett.*, 45(2), 475–482.

Brittenham, T. L., Neudecker, J. W., Rowley, J. C., and William, R. E. (1982). "Directional drilling equipment and techniques for deep, hot granite wells." *J. Pet. Technol.*, 34(7), 1421–1430.

Chen, X., Tan, C. P., and Detournay, C. (2003). "A study on wellbore stability in fracture rock masses with impact of mud infiltration." *J. Petrol. Sci. Eng.*, 38(3–4), 145–154.

Dezayes, C., Genter, A., and Valley, B. (2010). "Structure of the low permeable naturally fractured geothermal reservoir at Soultz." *C. R. Geosci.*, 342(7–8), 517–530.

Feng, X., Zhang, Z., and Sheng, Q. (2000). "Estimating mechanical rock mass parameters relating to the Three Gorges Project permanent shiplock using an intelligent displacement back analysis method." *Int. J. Rock Mech. Min. Sci.*, 37(7), 1039–1054.

Feng, X., Zhao, H., and Li, S. (2004). "A new displacement back analysis to identify mechanical geomaterial parameters based on hybrid intelligent methodology." *Int. J. Numer. Anal. Methods Geomech.*, 28(11), 1141–1165.

Gen, M., and Cheng, R. (1997). *Genetic algorithms and engineering design*, Wiley, New York.

Gokceoglu, C., Yesilnacar, E., Sonmez, H., and Kayabasi, A. (2004). "A neuro-fuzzy model for modulus of deformation of jointed rock masses." *Comput. Geotech.*, 31(5), 375–383.

Goldberg, D. E. (1989). *Genetic algorithm in search, optimization and machine learning*, 1st Ed., Addison-Wesley, Boston.

Goodman, R. E. (1970). "Deformability of joints." *Proc., Determination of the In Situ Modulus of Deformation of Rock*, ASTM, West Conshohoken, PA, 174–196.

Haftani, M., and Bohloli, B., Ellassi, M., and Talebi, B. (2008). "In-situ stress determination in Sabalan geothermal reservoir." *2nd IASME/WSEAS Int. Conf. on Geology and Seismology*, World Scientific and Engineering Academy and Society, Cambridge, U.K., 88–93.

Haimson, B., and Fairhurst, C. (1969). "In-situ stress determination at great depth by means of hydraulic fracturing." *11th U.S. Symp. on Rock Mechanics (USRMS)*, American Rock Mechanics Association, Alexandria, VA, 559–584.

Häring, M. O., Schanz, U., Ladner, F., and Dyer, B. C. (2008). "Characterization of the Basel 1 enhanced geothermal system." *Geothermics*, 37(5), 469–495.

Hossain, M. M., Rahman, M. K., and Rahman, S. S. (2002). "A shear dilation stimulation model for production enhancement from naturally fractured reservoirs." *SPE J.*, 7(2), 183–195.

Hesler, G. J., Zheng, Z., and Myer, L. R. (1990). "In-situ fracture stiffness determination." *Rock mechanics contribution and challenges*, W. Hustrulid and G. A. Johnson, eds., Balkema, Rotterdam, 405–411.

Huang, X., Haimson, B. C., Plesha, M. E., and Qiu, X. (1993). "An investigation of the mechanics of rock joints–Part 1. Laboratory investigation." *Int. J. Rock Mech. Min. Sci. Geomech. Abstr.*, 30(3), 257–269.

Jiang, X. W., Wan, L., Wang, X. S., Liang, S. H., and Hu, B. X. (2009). "Estimation of fracture normal stiffness using as transmissivity-depth correlation." *Int. J. Rock Mech. Min. Sci.*, 46(1), 51–58.

Jiang, Y., Xiao, J., Tanabashi, Y., and Mizokami, T. (2004). "Development of an automated servo-controlled direct shear apparatus applying a constant normal stiffness condition." *Int. J. Rock Mech. Min. Sci.*, 41(2), 275–286.

Jing, L., and Stephansson, O. (2007). *Fundamentals of discrete element methods for rock engineering: Theory and application, Developments in geotechnical engineering*, 1st Ed., Vol. 85, Elsevier, London.

Juliusson, E. (2012). "Characterization of fractured geothermal reservoirs based on production data." *SGP-TR-195*, Ph.D. thesis, Stanford Univ., Stanford, CA.

Koh, J., Roshan, H., and Rahman, S. S. (2011). "A numerical study on the long term thermo-poroelastic effects of cold water injection into naturally fractured geothermal reservoirs." *Comput. Geotech.*, 38(5), 669–682.

Kubik, W., and Lowry, P. (1993). "Fracture identification and characterization using cores, FMS, CAST, and Borehole camera: Devonian shale, Pike County, Kentucky." *SPE 25897, SPE Rocky Mountain/Low Permeability Reservoirs Symp. Proc.*, Society of Petroleum Engineers, Richardson, TX, 543–555.

Lewis, R. W., and Schrefler, B. A. (1998). *The finite element method in the static and dynamic deformation and consolidation of porous media*, Wiley, New York.

Li, S., Feng, X., and Hudson, J. A. (2013a). "ISRM suggested method for measuring rock mass displacement using a sliding micrometer." *Rock Mech. Rock Eng.*, 46(3), 645–653.

Li, S., Feng, X., Wang, C. Y., and Hudson, J. A. (2013b). "ISRM suggested method for rock fractures observations using a borehole digital optical televiewer." *Rock Mech. Rock Eng.*, 46(3), 635–644.

Ljunggren, C., Chang, Y., Janson, T., and Christiansson, R. (2003). "An overview of rock stress measurement methods." *Int. J. Rock Mech. Min. Sci.*, 40(7–8), 975–989.

Magnusdottir, L., and Horne, R. N. (2011). "Characterization of fractures in geothermal reservoirs using resistivity." *Proc., 36th Workshop on Geothermal Reservoir Engineering*, Stanford Univ., Stanford, CA, 1–7.

Main, I. G., Meredith, P. G., Sammonds, P. R., and Jones, C. (1990). "Influence of fractal flaw distributions on rock deformation in the brittle field in deformation mechanisms." *Deformation mechanisms, rheology and tectonics, Geological Society of London special publication No. 54*, R. J. Knipe and E. H. Rutter, eds., 81–96.

McCulloch, W. S., and Pitts, W. H. (1943). "A logical calculus of the ideas immanent in nervous activity." *Bull. Math. Biol.*, 5(4), 115–133.

McDermott, C., and Kolditz, O. (2006). "Geomechanical model for fracture deformation under hydraulic, mechanical and thermal loads." *Hydrogeol. J.*, 14(4), 485–498.

Moos, D., and Zoback, M. D. (1990). "Utilization of observations of well bore failure to constrain the orientation and magnitude of crustal stresses: Application to continental, deep sea drilling project, and ocean drilling program boreholes." *J. Geophys. Res.*, 95(B6), 9305–9325.

Morris, J. P. (2012). "A numerical investigation of the scaling of fracture stiffness." *ARMA 12-610*, *46th U.S. Rock Mechanics/Geomechanics Symp.*, American Rock Mechanics Association, Alexandria, VA, 52–59.

Nassir, M., Settari, A., and Wan, R. (2010). "Joint stiffness and deformation behavior of discontinuous rock." *J. Can. Pet. Technol.*, 49(9), 78–86.

Nicolson, J. P. W., and Hunt, S. P. (2004). "Distinct element analysis of borehole instability in fractured petroleum reservoir seal formation." *SPE 88610*, *SPE Asia Pacific Oil and Gas Conf. and Exhibition*, Society of Petroleum Engineers, Richardson, TX, 231–240.

Nikravesh, M., Aminzadeh, F., and Zadeh, L. A. (2003). *Soft computing and intelligent data analysis in oil exploration*, Elsevier Science B. V., Boston.

Noorzad, A., and Aminpoor, M. (2008). "Effect of joint stiffness values on stresses of jointed rocks." *5th Asian Rock Mechanics Symp.*, Int. Society for Rock Mechanics, Lisbon, Portugal, 437–444.

Pichler, B., Lackner, R., and Mang, H. A. (2003). "Back analysis of model parameters in geotechnical engineering by means of soft computing." *Int. J. Numer. Methods Eng.*, 57(14), 1943–1978.

Rutqvist, J., and Stephansson, O. (1996). "A cyclic hydraulic jacking test to determine the in situ stress normal to a fracture." *Int. J. Rock Mech. Min. Sci. Geomech. Abstr.*, 33(7), 695–711.

Rutqvist, J., and Stephansson, O. (2003). "The role of hydromechanical coupling in fractured rock engineering." *Hydrogeol. J.*, 11(1), 7–40.

Sahoo, G. B., and Ray, C. (2006). "Flow forecasting for a Hawaiian stream using rating curves and neural networks." *J. Hydrol. (Amst.)*, 317(1–2), 63–80.

Sharifzadeh, M., and Karegar, S. (2007). "Hydromechanical analysis of the effect of fracture properties on tunnel inflow." *Proc., 1st Canada–US Rock Mechanics Symp.*, Taylor & Francis, London, 441–445.

Sheridan, J. M., and Hickman, S. H. (2004). "In situ stress, fracture, and fluid flow analysis in well 38C-9 and enhanced geothermal system in the COSO geothermal field." *Proc., 29th Workshop on Geothermal Reservoir Engineering*, Stanford Univ., Stanford, CA, 417–426.

Universal Distinct Element Code (UDEC) 5.0 [Computer software]. Minneapolis, Itasca Consulting Group.

Valley, B., and Evans, K. F. (2007). "Stress state at Soultz-sous-Forets to 5 km depth from wellbore failure and hydraulic observations." *32nd Workshop on Geothermal Reservoir Engineering*, Stanford Univ., Stanford, CA, 329–338.

Watanabe, K., and Takahashi, H. (1995). "Fractal geometry characterization of geothermal reservoir facture networks." *J. Geophys. Res.*, 100(B1), 521–528.

White, A. J., Traugott, M. O., and Swarbrick, R. E. (2002). "The use of leak-off tests as means of predicting minimum in situ stress." *Petrol. Geosci.*, 8(2), 189–193.

Witherspoon, P. A., Wang, J. S. Y., Iwai, K., and Gale, J. E. (1980). "Validity of cubic law for fluid flow in a deformable rock fracture." *Water Resour. Res.*, 16(6), 1016–1024.

Yang, Z., Crosby, D. G., Akgun, F., Khurana, A. K., and Rahman, S. S. (1997). "Investigation of the factors influencing hydraulic fracture initiation in highly stressed formations." *SPE Asia Pacific Oil and Gas Conf. and Exhibition*, Society of Petroleum Engineers, Richardson, TX, 149–161.

Yilmaz, I., and Yuksek, A. G. (2008). "An example of artificial neural network (ANN) application for indirect estimation of rock parameters." *Rock Mech. Rock Eng.*, 41(5), 781–795.

Yin, S., Towler, B. F., Dusseault, M. B., and Rothenburg, L. (2010). "Fully coupled THMC modeling of wellbore stability with thermal and solute convection considered." *Transp. Porous Media*, 84(3), 773–798.

Yuan, Y.-G., Abousleiman, Y., and Roegiers, J.-C. (1995). "Fluid penetration around a borehole under coupled hydro-electro-chemico-thermal potentials." *46th Annual Technical Meeting of the Petroleum Society of CIM*, Canadian Institute of Mining, Metallurgy and Petroleum, Westmount, QC, Canada, 72–95.

Zhang, S., and Yin, S. (2013). "Reservoir geomechanical parameters identification based on ground surface movements." *Acta Geotech.*, 8(3), 279–292.

Zoback, M. D. (2007). *Reservoir geomechanics*, Cambridge University Press, Cambridge, U.K.